Int. J. Electrochem. Sci., 12 **(2017)** 10390 – 10401, doi: 10.20964/2017.11.45

International Journal of
ELECTROCHEMICAL
SCIENCE
www.electrochemsci.org

A Novel H_2O_2 Biosensor Based On the composite of MP-11 encapasulated in PCN-333(Al)-Graphene Oxide

Mengli Xu, Yuan Shen, Linyu Wang, Coucong Gong and Shouhui Chen *

College of Chemistry and Chemical Engineering, Jiangxi Normal University, 99 Ziyang Road, Nanchang 330022, China.
*E-mail: csh2k@sina.com

Received: 10 May 2017 / *Accepted:* 22 August 2017 / *Published:* 12 October 2017

In this work, a novel H_2O_2 biosensor was developed based on the composites of microperoxidase-11 (MP-11) encapsulated in graphene oxide (GO)-PCN-333 (Al) (PCN stands for porous coordination network, one of the metal-organic frameworks). The PCN-333(Al) firmly and uniformly grew on the surface of GO sheet with large specific surface and excellent electrical conductivity, which provided a lots of pores for the encapsulation of MP-11 in the composites and selectively accumulated analytes into its mesopores to improve the selectivity of enzymatic reaction. The MP-11 molecules might freely move through mesopores of PCN-333 (Al) to maintain bioactivity, which remarkably enhanced the mass transfer rate and quickened the electron transfer for electrochemical biosensors. Scanning electron microscopy was used to characterize the GO and PCN-333(Al)-GO composites. Cyclic voltammetry and differential pulse voltammetry were used to characterize the electrochemical behaviors and performance of the H_2O_2 biosensor. The target electrode showed excellent performance with a wide linear range from 10 μM to 800 μM, a low detection limit of 3 μM, good stability and high selectivity, which was superior to some other H_2O_2 biosensors.

Keywords: Electrochemical biosensor; Graphene oxide; PCN-333 (Al); Microperoxidase-11; H_2O_2; Metal-organic frameworks

1. INTRODUCTION

Recently, the quantitative detection of hydrogen peroxides (H_2O_2) [1-5] has attracted more and more attention. Owing to H_2O_2 as a natural byproduct of oxidative metabolism, it plays an essential role in versatile biology in vivo[6-9]. Hence, it was crucial to develop reliable and sensitive methods for H_2O_2 detection. According to literature reports, the enzyme-based electrochemical H_2O_2 biosensors [8, 10] such as cytochrome *c* (Cyt *c*), microperoxidase-11(MP-11), horseradish peroxidase (HRP) and myoglobin (Mb) demonstrated the following advantages: high selectivity, low cost, good sensitivity

and simplified operation. However, considering that the enzymes were vulnerable to environment and degenerate inactivation when immobilized on the electrode surface, which lead to a weak stability and a bad repeatability for the performance of enzyme-based biosensors. Hence, it was crucial for H_2O_2 biosensors to search for a new method to firmly load enzymes on the constructed electrode surface [11, 12] to avoid aggregation.

Metal-organic frameworks (MOFs) has properties of ultra-high porosity, tunable pore size and shape, ordered structure, adjustable surface functionality and excellent catalytic activity[13-18]. And it was considered to be a promising platform for immobilization of various catalysts[19, 20], such as nanoparticles[21, 22], enzymes[23-25] and metal complexes[26]. Especially used as enzymes supporting, MOFs can not only encapsulate enzymes into its pores to avoid the stack of enzyme, but also selectively accumulate analytes into its pores to benefit selectivity [10, 23, 27]. For example, PCN-333 (Al, Fe) MOFs[28-30] (PCN stands for porous coordination network) possessed high stability in aqueous solution with pH values from 3 to 9, which made it an extraordinary encapsulation supporting for different size biomolecules, including Cyt *c*, HRP and MP-11. Tb@mesoMOFs[23] was also used as platform to load MP-11 and Mb bioprotein molecules in the pores to maintain catalytic activity. The graphene oxide (GO) sheets, two-dimensional carbon material, possess large specific surface area, wide electrochemical window and excellent conductivity[31, 32], which was regarded as a good supporting to adsorb metal nanomaterials or enzyme for biosensors[33-36]. MP-11 is a heme protein [10, 24] with small size and is obtained via proteolytic digestion of Cyt *c*. It consists of eleven amino acids and a covalently linked Fe^{III}- protoporphyrin IX heme[37]. The centre of redox MP-11 protein molecules can catalyze the reduction of H_2O_2 [38, 39].

In this work, a novel H_2O_2 biosensor was successfully constructed based on PCN-333(Al)-GO nanocomposite which was used to load MP-11 molecules for catalyzing H_2O_2 reduction. Due to the lamellar fold structure, large specific surface area and excellent electrical conductivity, GO can provide large amounts of active sites for PCN-333(Al) firmly and uniformly grown on its surface. MP-11 was immobilized on the PCN-333(Al)-GO to avoid their aggregation and might freely move through mesopores for enhancing bioactivity. Furthermore, PCN-333(Al) selectively accumulated the analytes into its mesopores, which improved the selectivity of enzymatic reaction. Hence, the electron transfer between MP-11 and modified electrode could improve to enhance the performance of H_2O_2 biosensors with a wide linear range, high sensitivity and low detection limit.

2. EXPERIMENTAL

2.1. Chemicals and materials

MP-11 (90%), 4, 4′, 4″ -s-triazine-2, 4, 6-triyl-tribenzoic acid (H_3TATB, 95%) and trifluoroacetic acid (TFA, 99%) were purchased from Sigma-Aldrich. Aluminium trichloride hexahydrate ($AlCl_3 \cdot 6H_2O$), N, N-dimethyl formamide (DMF, AR) and H_2O_2 (AR, 30 wt.% in H_2O) were purchased from Aladdin. Glucose, surcrose, ascorbic acid (AA), NaCl, KCl, cysteine, graphite powder (spectrum pure) and other reagents were purchased from Sinopharm Chemical Reagent Co.,

Ltd (Shanghai, China). The 0.2 M phosphate buffer solution (PBS) was obtained from 0.2 M NaH_2PO_4 and 0.2 M Na_2HPO_4. The MP-11 solution (1 mg mL^{-1}) was prepared in 0.2 M PBS (pH 7.0) and stored in 4 °C. All solutions were prepared with ultra-pure water purified by a Millipore-Q System (ρ≥18.2 MΩ cm^{-1}).

2.2. Synthesis of the PCN-333(Al)-GO nanocomposites

The graphene oxide (GO) of lamellar fold was synthesized according to Hummers' method. Then, 2 mg of H_3TATB and 8 mg of $AlCl_3 \cdot 6H_2O$ were dissolved in 2 mL of DMF at ambient temperature. And then, 200 μL of TFA and the GO aqueous solution (0.1 mg mL^{-1}) were added into the above solution in turn. After that, the mixture was heated at 135 °C in an oven for 12 h, which resulted in the formation of PCN-333(Al)[1, 28] on the surface of GO. The as-synthesis PCN-333(Al)-GO composite was alternately rinsed with ethanol and ultra-pure water for three times, and dried at 60 °C for the next use.

2.3. Preparation of MP-11/PCN-333(Al)-GO/GCE electrode

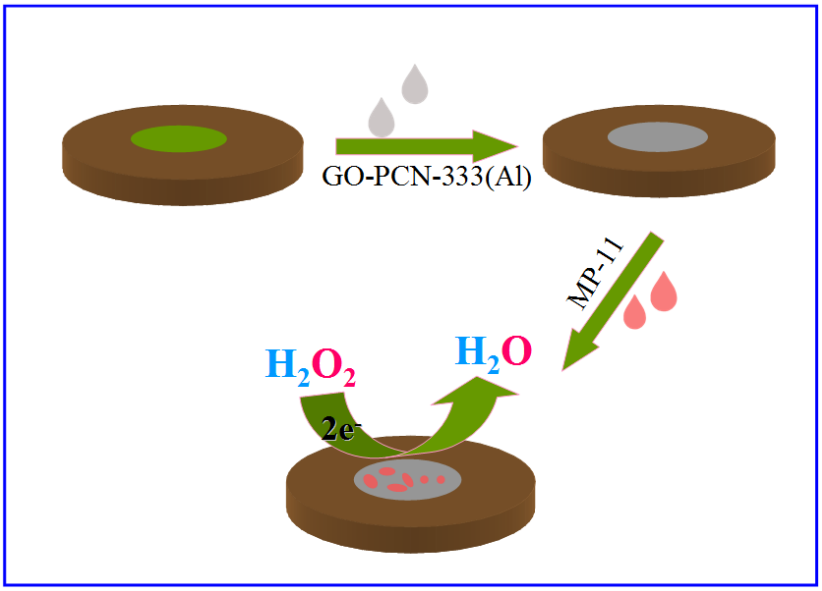

Figure 1. Schematic illustration of the stepwise fabrication process and testing principle of the novel H_2O_2 electrochemical biosensor

The suspension of PCN-333(Al)-GO composite (2 mg mL^{-1}) was dropped on the surface of polished glassy carbon electrode (GCE). Finally, the as-prepared MP-11/GO-PCN-333 (Al) /GCE was obtained by immersing PCN-333(Al)-GO/GCE in a MP-11 solution (1 mg mL^{-1}) for 12 h and then dried in air. To further improve the performance of the electrode, the resulted electrode was rinsed with fresh buffer solution for several times to remove the weakly absorbed molecules and then dried in air. The detailed process of the MP-11/PCN-333(Al)-GO/GCE was shown in Fig. 1.

2.4. Instrumentations

A three-electrode system of a platinum wire as the counter electrode, a saturated calomel electrode (SCE) as the reference electrode and a bare or modified GCE as the working electrode was used. Cyclic voltammograms (CVs) were operated in 0.1 M KCl solution containing 5.0 mM $Fe(CN)_6^{3-/4-}$ at room temperature or N_2-saturated 0.2 M PBS (pH 7.0). Electrochemical impedance spectroscopy (EIS) was performed in 0.1 M KCl solution containing 5.0 mM $Fe(CN)_6^{3-/4-}$ at open circuit potential in the frequency range from 0.01 Hz to 105 Hz with the amplitude 5 mV. Differential pulse voltammetry (DPV) was performed in N_2-saturated 0.2 M PBS (pH 7.0) with amplitude of 50 mV and pulse width of 0.2 s. The amperometric experiment was carried out under a continuous stirring. Scanning electron microscopy (SEM) images were performed using a HITACHI S-3400N SEM at an accelerating voltage of 15 kV. All electrochemical experiments were carried out using a CHI 760D electrochemical workstation (Shanghai, China).

3. RESULTS AND DISCUSSION

3.1 Characterization of PCN-333(Al)-GO/GCE

As shown in Fig. 2, SEM was firstly used to characterize morphology of the PCN-333(Al)-GO composites. Compared with as-synthesized GO, which was lamellar fold and smooth (Fig. 2A), the surface of PCN-333(Al)-GO composites became thicker and rougher, and there was many uniform upheaval on it (Fig. 2B). The figures clearly indicated that PCN-333(Al) had successfully grew on the surface of GO, which would vastly enlarge the number of immobilized enzyme and improve the electrical conductivity of PCN-333(Al)-GO composites.

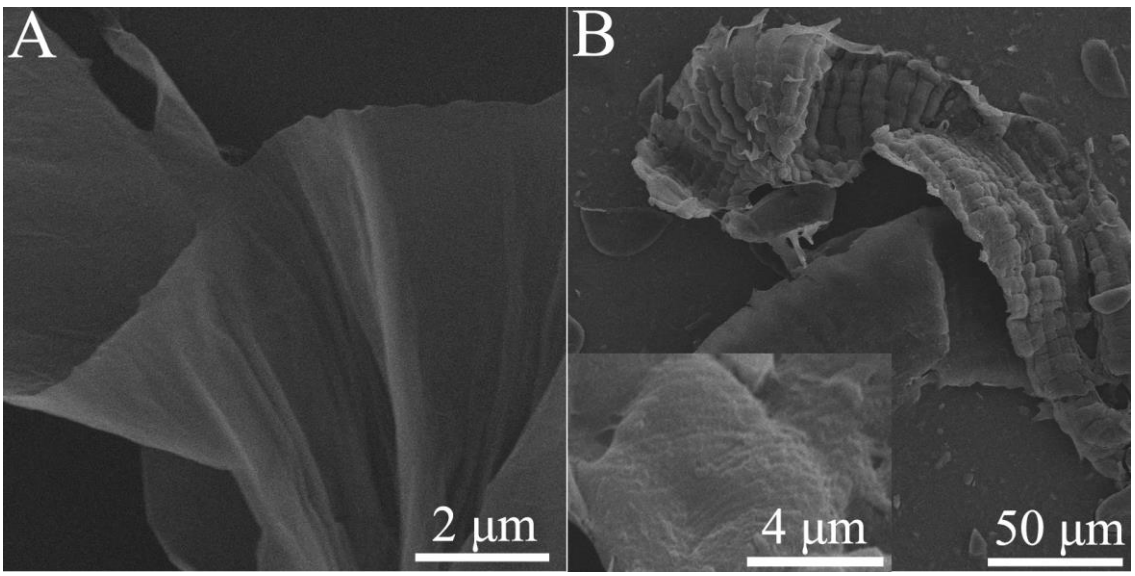

Figure 2. SEM images of the GO (A) and the PCN-333 (Al)-GO (B). Inset was the high-resolution SEM image.

3.2 Electrochemical behaviors of the MP-11/PCN-333(Al)-GO/GCE

The modified process of the resulted MP-11/PCN-333(Al)-GO/GCE was monitored by CVs and EIS in 0.1 M KCl solution containing 5.0 mM $Fe(CN)_6^{3-/4-}$ at room temperature (Fig. 3A and Fig. 3B). It showed that a pair of typical redox peak of $Fe(CN)_6^{3-/4-}$ exsited for bare GCE (curve a). Then the redox peak current declined and peak-to-peak potential separation (ΔE_p) increased after the PCN-333(Al)-GO nanocomposites modified on the GCE (curve b). Considering that poor conductivity of PCN-333(Al), it was possible for PCN-333(Al)-GO to hinder the electron transfer of $Fe(CN)_6^{3-/4-}$. Furthermore, the redox peak current markedly declined and the ΔEp increased after MP-11 molecules were loaded on the PCN-333(Al)-GO/GCE (curve c), which could be explained that the MP-11 molecules as biological protein enzymes were successfully encapsulated into the PCN-333(Al)-GO/GCE.

As shown in Fig. 3B, the resistance of charge transfer (R_{ct}) for the bare GCE was calculated to be 40 Ω (curve a), while that of PCN-333(Al)-GO/GCE and MP-11/PCN-333(Al)-GO/GCE increased to 400 Ω (curve b) and 800 Ω (curve c), respectively. Hence, the variation trend of EIS was consistent with that of CVs. The inset in Fig. 3B was the Randles equivalence circuit model used to fit EIS data. In summary, it strongly demonstrated that multistep modification process of non-electroactive molecules hindered the electron transfer of $Fe(CN)_6^{3-/4}$. Besides, Fig. 4A showed the CVs response of MP-11/PCN-333(Al)-GO/GCE with different scan rate controlled in 0.2 M N_2-staturated PBS (pH 7.0). As shown in Fig. 4B, the redox peak current density linearly increased as scan rate raised from 100 mV s^{-1} to 1000 mV s^{-1}. It suggested that the electron transfer process of MP-11 encapsulated in the mesopores of PCN-333(Al)-GO/GCE was essentially a surface adsorption control process.

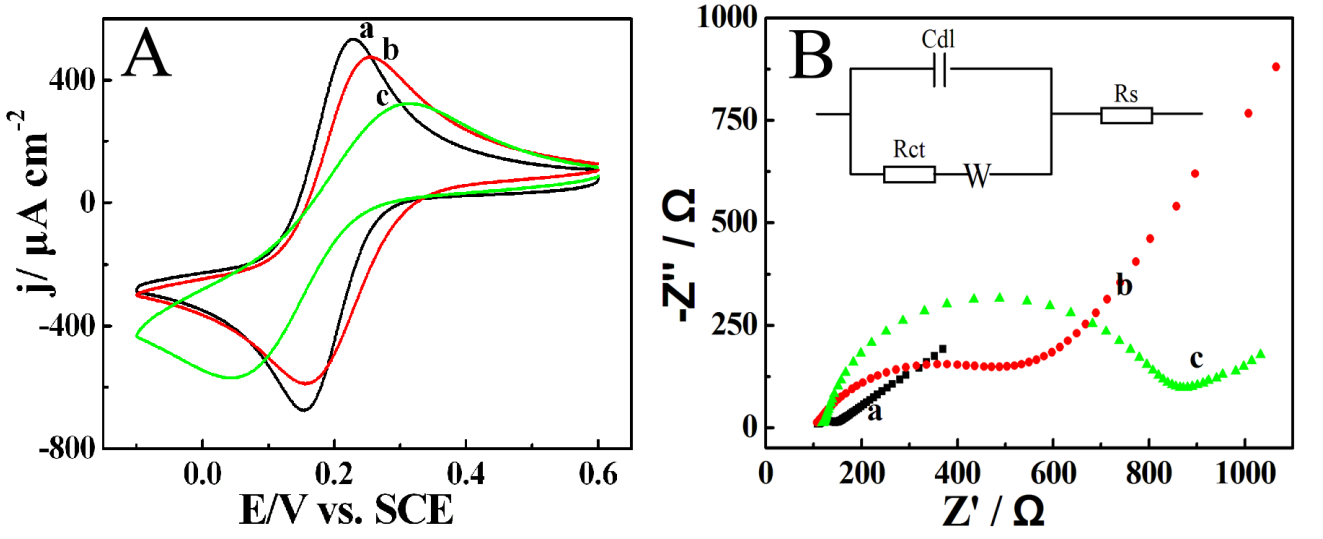

Figure 3. CVs (A) and EIS (B) of various electrodes in 0.1 M KCl aqueous solution containing 5 mM $Fe(CN)_6^{3-/4-}$: GCE (curve a, black line), PCN-333(Al)-GO/GCE (curve b, red line) and MP-11/PCN-333(Al)-GO /GCE (curve c, green line). Inset is the Randles circuit.

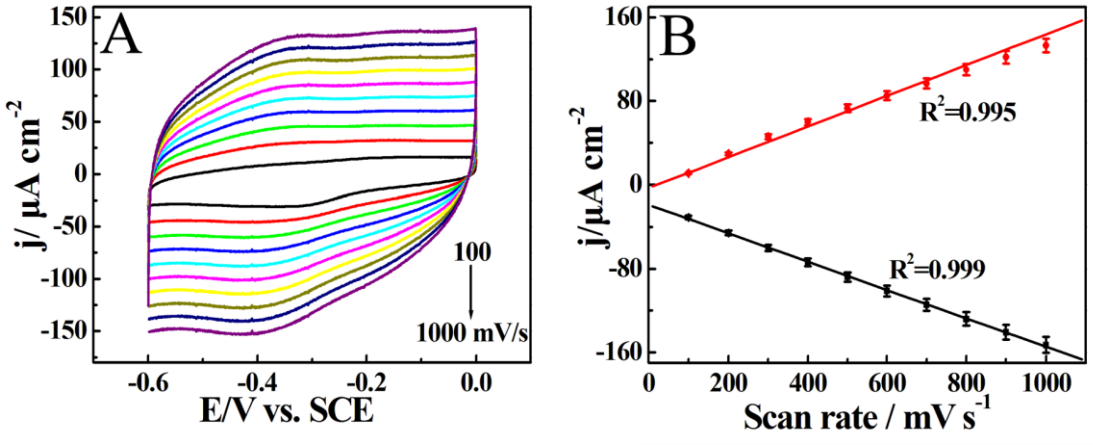

Figure 4. (A) CVs of MP-11 /PCN-333 (Al)-GO/GCE at different scan rates (from inner to outer: 100, 200, 300, 400, 500, 600, 700, 800,900, and 1000 mV s-1). (B) Plot of cathodic and anodic peak current for MP-11/PCN-333 (Al)-GO/GCE versus scan rate.

3.3. Optimization conditions of electrochemical detection for H_2O_2

As a heme protein, the MP-11 molecule can efficiently catalyze reduction of H_2O_2. Correspondingly, the reduction peak current of MP-11 would increase with the addition of H_2O_2. Herein, the H_2O_2 biosensor was constructed. Since the structure of GO was lamellar fold, it possessed large specific surface area and excellent electrical conductivity when compared with PCN-333(Al) MOFs of octahedron structure. Accordingly, the GO can provide a large number of active sites for PCN-333(Al) MOFs firmly and uniformly grown on the surface and also strengthened the electrical conductivity of electrode materials, which was beneficial to enhance the mass and electron transfer rate for electrochemical biosensors. Moreover, when the MP-11molecule, a biological protein enzyme, was encapsulated into the PCN-333(Al)-GO/GCE, it might freely move through mesopores, and keep well with its bioactivity to catalyze reduction of H_2O_2. Furthermore, the electron transfer between MP-11 and the supporting electrode was so fast that the electrochemical performances of the biosensors were significantly improved. The enzymatic reaction mechanism was listed in the following [40, 41]:

$$2\text{MP-11-Fe(II)} + H_2O_2 + 2H^+ \rightarrow 2H_2O + 2\text{MP-11-Fe (III)} \quad (1)$$

In order to control the optimal electrochemical performance of H_2O_2 biosensors, some important experimental factors referred to the catalysis behavior of MP-11/PCN-333(Al)-GO/GCE would be explored. Firstly, the amount of GO doped in PCN-333(Al)-GO composites which could influence the loaded amounts of PCN-333(Al) MOFs on the surface was optimized. When the amount of other relative regents kept constant such as H_3TATB (2 mg) and $AlCl_3 \cdot 6H_2O$ (8 mg) and maintained reaction time for 48 h in 135 °C, it could be clearly observed that the catalytic reduction peak current increased with GO concentration varied from 0 to 0.1 mg mL^{-1}, after that, the peak current gradually declined with the GO concentration continuously increased to 0.5 mg mL^{-1} (Fig. 5A). So, it indicated that the optimal concentration of GO doped in PCN-333(Al)-GO composite was about 0.1 mg mL^{-1}, which was used in the following experiments. Secondly, the catalytic reduction peak current of MP-11 gradually increased with the reaction time varied from 8 h to 12 h (Fig. 5B), and then decreased from

12 h to 16 h, which demonstrated the reaction time of 12 h was optimal to construct the H_2O_2 biosensor. It might be result from the size or amounts of PCN-333(Al) MOFs excessively enlarged and became dense after 12 h, which lead to the dropping of the modified electrode's performance.

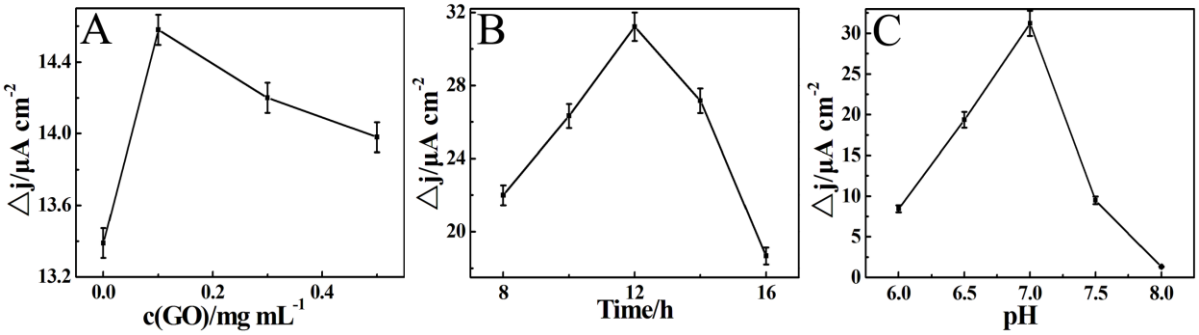

Figure 5. The effects of GO concentration (A), reaction time in mixed solution (B) in N_2-satruated 0.2 M PBS (pH 7.0), and different pH(C) on the catalytic cathodic peak current for MP-11/PCN-333 (Al)-GO/GCE with 0.3 mM H_2O_2.

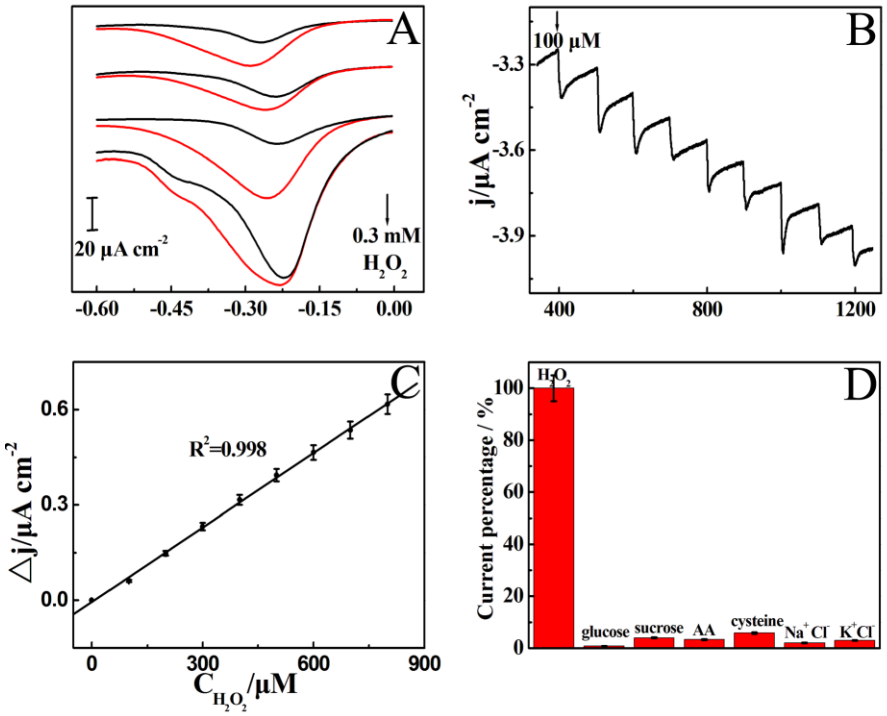

Figure 6. (A) DPV responses of MP-11/PCN-333(Al)/GCE, MP-11/GO/GCE, MP-11/PCN-333(Al)-GO/GCE and MP-11/GCE (from up to down) in 0.2 M N_2-satruated PBS (pH 7.0) without (black line) and with 0.3 mM H_2O_2 (red line). (B) Amperometric responses of MP-11/PCN-333(Al)-GO/GCE in a stirring 0.2 M N_2-satruated PBS (pH 7.0) with different H_2O_2 concentration at -0.25 V. (C) The amperometric calibration curves of MP-11/PCN-333(Al)-GO/ GCE for H_2O_2 detection. (D) DPV responses of MP-11/PCN-333(Al)-GO/GCE to different chemicals: 5-flod of glucose, sucrose, AA, Na^+, Cl^-, K^+ and cysteine in 0.2 M N_2-satruated PBS (pH 7.0).

Simultaneously, as a biological protein enzyme, MP-11 might aggregate and not be firmly encapsulated into the surface of PCN-333(Al)-GO/GCE electrode, which had negative effects on the mass transfer and blocked the electron transfer between MP-11 molecules and the resulting electrode. Besides, the pH value of the buffer solution would influence the bioactivity of MP-11 enzyme on the surface of constructed electrode. As shown in Fig. 5C, the catalytic reduction peak current of MP-11 reached the maximum value when the pH value was 7.0. It was easy for enzyme to degenerate inactivation under excessively acidic and alkaline condition.

Based on optimized experimental parameters of the H_2O_2 biosensor, the DPV response of various modified electrode in 0.2 M N_2-saturated PBS (pH 7.0) without (black line) and with 0.3 mM H_2O_2 (red line) was shown in Fig. 6A. All of the reduction peak currents of MP-11 increased as the addition of 0.3 mM H_2O_2, and the catalytic current of MP-11/PCN-333(Al)-GO/GCE was obviously larger than that of MP-11/GCE, MP-11/GO/GCE and MP-11/PCN-333(Al)/GCE, which strongly indicated PCN-333(Al)-GO composites was the key to construct biosensors.

Table 1. Comparison of the performance of novel H_2O_2 biosensors based on the MP-11/PCN-333(Al)-GO/GCE electrode with other H_2O_2 biosensors.

Modified Electrode	Potential (vs. Hg_2Cl_2/Hg)	Linear range/(μM)	Detection limit/(μM)	Ref.
MP-11/DMPG[a]-AuNPs/PDDA-G[b]/GCE	-0.4 V	20-280	2.6	[42]
MP-11/ITO[c]	-0.38 V	2-600	6.0	[43]
MP-11/MGN-CHIT[d]/Au	-0.35 V	2.5-135	2.0	[44]
MP-11/PEI[e] film	-	25.00-120	5.7	[45]
MP-11/PCN-333 (Al)/3D-KSCs	-0.3 V	0.39-1725	0.127	[1]
MP-11/Tb@mesoMOFs/CHIT-AuNPs/3D-KSCs	-0.4 V	3.02-640	0.996	[46]
MP-11/PCN-333(Al)-GO/GCE	-0.25 V	10-800	3	This work

[a] DMPG : 1,2-dimyristoyl-sn-glycero-3-phosphatidil glycerol.
[b] PDDA-G: Diallyldimethylammonium chloride-modified-graphene nanosheets.
[c] ITO: indium-doped tin oxide sheet
[d] MGN-CHIT: multilayer graphene nanosheets chitosan
[e] PEI: poly(ethylene imine)

Fig. 6B showed the amperometric responses of MP-11/PCN-333(Al)-GO/GCE in a stirring 0.2 M N_2-satruated PBS (pH 7.0) with different H_2O_2 concentration at -0.25 V. The catalytic reduction peak current of MP-11 gradually linearly raised as the addition of H_2O_2 increased from 10 μM to 800 μM (R^2 = 0.998, n = 8), and the detection limit was calculated to be *3* μM (S/N = 3) for MP-11/PCN-333(Al)-GO/GCE. The sensitivity of the resulted biosensor was 7 μA mM^{-1} cm^{-2}. Compared with other MP-11 based H_2O_2 biosensor[1,42-46] (Table 1), the detection limit of MP-11/PCN-333(Al)-GO/GCE electrode was lower than that of MP-11/PEI film[45] and MP-11/ITO electrode[43]. It might

be that PCN-333(Al) firmly grew on the surface of GO sheet, provided more mesopores to encapsulate electroactive substances as supporting materials, and enhanced electrical conductivity than that of PEI film or ITO sheet. And MP-11 might move freely in the pore of PCN-333(Al), keep its biological activity well, and enhance the mass transfer and electron transfer rate. Moreover, the as-prepared electrode had a wider linearity range (10-800 μM) among the electrodes in Table 1, which should be the effect of PC N-333(Al) selectively accumulating analytes into its mesopores, as well as the lower detection limit. Although the detection limit of as-prepared electrode was higher than that of other MP-11 based electrodes (in Table 1), its work potential was just -0.25 V, which was more helpful to reduce interferences during the detection process. The lower work potential might be ascribed to the N-containing function group in PCN-333(Al). Above all, the good catalytic performance of novel H_2O_2 sensor based on MP-11/PCN-333(Al)-GO/GCE, should be ascribed to the large specific surface, excellent electrical conductivity, quick electron transfer and mass transfer rate between the modified electrode and signal-generating species.

In order to evaluate the feasibility of the MP-11/PCN-333(Al)-GO/GCE electrode in real samples, it was used to detect the content of H_2O_2 in a commercial contact lens care solution. As pretreatment, the sample was firstly diluted by 0.2 M PBS (pH 7.0) before determination. Then, different diluted samples were performed by DPV with the standard H_2O_2 solution added into the testing systems subsequently. As shown in Table 2, the recovery capability for different samples was between 85.0% and 112.5%, as well as the relative standard deviation was less than 5.75 % by three resulted successive electrodes under the same testing condition. Compared with the concentration of H_2O_2 calculated for standard addition method, the result confirmed that the constructed H_2O_2 biosensor based on MP-11/PCN-333(Al)-GO/GCE electrode was reliable and acceptable for detection in some practical samples.

Table 2. Determination of H_2O_2 in diluted commercial contact lens solutions

Sample (mM)	Diluted Samples (mM)	Added (mM)	Determined by MP-11/PCN-333(Al)-GO/GCE electrode (mM)	Recovery (%)	RSD (%, n=3)
0.8	0.04	0.1	0.13	90.0	5.75
	0.08	0.1	0.19	110.0	4.08
	0.16	0.2	0.33	85.0	3.41
	0.40	0.2	0.65	112.5	3.93

3.4 Selectivity, reproducibility and stability of the constructed H_2O_2 biosensor

DPV response of the constructed H_2O_2 biosensor to reduction peak current was measured in the presence of common interfering materials, such as glucose, sucrose, AA, Na^+, Cl^-, K^+ and cysteine. And the results showed that the interference of organic compounds, including glucose, sucrose, AA and cysteine, was poor (<5%) in a 5-fold H_2O_2 concentration (0.3 mM), in which that of glucose was below 1%. Other inorganic substance, such as Na^+, K^+ and Cl^-, made no obvious interference (<3%) in a 5-fold H_2O_2 concentration (Fig. 6D). It indicated that the electrode of MP-11/PCN-333(Al)-GO/GCE possessed good selectivity for H_2O_2 detection. Furthermore, after the biosensors was stored for 48 h at 4 °C, the catalytic current response of the biosensor to 0.3 mM H_2O_2 only declined 3.8% compared with that of the electrode before storing. The relative standard deviation (RSD) was calculated to be 6.5% according to the experiment data of five as-prepared electrodes used successively to detect 0.3 mM H_2O_2 under the same condition. Hence, these novel H_2O_2 biosensors exhibited excellent stability and selectivity. The superior selectivity, reproducibility and stability of the MP-11/PCN-333(Al)-GO/GCE electrode might be ascribed to the large amount of MP-11 enzyme firmly encapsulated into PCN-333(Al)-GO composites, which made the electrode exhibit excellent catalytic bioactivity than that of other modified electrodes. Moreover, PCN-333(Al)-GO composites could also selectively accumulate target analytes toward H_2O_2 in some degree.

4. CONCLUSIONS

In summary, a novel electrochemical H_2O_2 biosensor was constructed based on the MP-11/PCN-333(Al)-GO/GCE. The GO sheets were used as a support provided huge specific surface for the growth of PCN-333 (Al) on the surface uniformly, which not only further benefited the immobilization quantities of bioactivity enzyme, but also selectively accumulated analytes into its mesopores to improve the selectivity of enzymatic reaction. The MP-11 enzyme was firmly encapsulated into the mesopores of PCN-333 (Al) and might move freely to maintain biological activity well, which remarkably enhanced the mass transfer rate and quickened the electron transfer for electrochemical sensor. Hence, the constructed target electrode for the detection of H_2O_2 exhibited good catalytic performance with a wide linear range from 10 μM to 800 μM, a low detection limit of 3 μM, good stability and high selectivity. And the PCN-333(Al)-GO could not only be suitable for immobilizing MP-11 but also be applicable for encapsulating other enzyme. Correspondingly, the work set a good example to develop biosensor on the basis of MOFs and MP-11.

ACKNOWLEDGEMENTS
This work was financially supported by National Natural Science Foundation of China (21465014, 21465015 and 21665012), Natural Science Foundation of Jiangxi Province (20143ACB21016), the Ground Plan of Science and Technology Projects of Jiangxi Educational Committee (KJLD14023), and Scientific Research Foundation of Jiangxi Education Commission (GJJ160288), Graduate Student Innovation Foundation of Jiangxi Province.

References

1. C. Gong, Y. Shen, J. Chen, Y. Song, S. Chen, Y. Song and L. Wang, *Sens. Actuators, B,* 239 (2017) 890.
2. M. T. Tajabadi, M. Sookhakian, E. Zalnezhad, G. H. Yoon, A. M. S. Hamouda, M. Azarang, W. J. Basirun and Y. Alias, *Appl. Surf. Sci.*, 386 (2016) 418.
3. M. S. Hammadi, K. Cheng and W. W, J. Ni, *Sens. Mater.*, 1 (2017) 95.
4. Y. Shu, J. Chen, Q. Xu, Z. Wei, F. Liu, R. Lu, S. Xu and X. Hu, *J. Mater. Chem. B*, 5 (2017) 1446.
5. J. Balamurugan, T. D. Thanh, G. Karthikeyan, N. H. Kim and J. H. Lee, *Biosens. Bioelectron.*, 89 (2017) 970.
6. Z. Chen, D. Sun, Y. Zhou, J. Zhao, T. Lu, X. Huang, C. Cai and J. Shen, *Biosens. Bioelectron.*, 29 (2011) 53.
7. J. Bai and X. Jiang, *Anal. Chem.*, 85 (2013) 8095.
8. A. Yagati and J. Choi, *Electroanalysis.*, 26 (2014) 1259.
9. R. Zhang and W. Chen, *Biosens. Bioelectron.*, 89 (2017) 249.
10. Y. Astuti, E. Topoglidis and J. R. Durrant, *Anal. Chim. Acta*, 686 (2011) 126.
11. X. Wu, M. Hou and J. Ge, *Catal. Sci. Technol.*, 5 (2015) 5077.
12. K. S. Prasad, C. Walgama and S. Krishnan, *RSC Adv.*, 5 (2015) 11845.
13. M. Jin, Z. L. Mou, R. L. Zhang, S. S. Liang and Z. Q. Zhang, *Biosens. Bioelectron.*, 91 (2017) 162.
14. C. S. Liu, C. X. Sun, J. Y. Tian, Z. W. Wang, H. F. Ji, Y. P. Song, S. Zhang, Z. H. Zhang, L. H. He and M. Du, *Biosens. Bioelectron.*, 91 (2017) 804.
15. Q. G. Zhai, X. Bu, X. Zhao, D. S. Li and P. Feng, *Accounts. Chem. Res.*, 50 (2017) 407.
16. S. S. Nadar and V. K. Rathod, *Int. J. Biol. Macromol.*, 95 (2017) 511.
17. I. Nath, J. Chakraborty and F. Verpoort, *Chem. Soc. Rev.*, 45 (2016) 4127.
18. Y. Bai, Y. Dou, L.-H. Xie, W. Rutledge, J.-R. Li and H.-C. Zhou, *Chem. Soc. Rev.*, 45 (2016) 2327.
19. A. Nagaraj and D. Amarajothi, *J. Colloid Interface Sci.*, 494 (2017) 282.
20. P. Mahato, A. Monguzzi, N. Yanai, T. Yamada and N. Kimizuka, *Nat. Mater.*, 16 (2016) 153.
21. W. Lu, X. Qin, A. M. Asiri, A. O. Al-Youbi and X. Sun, *Analyst*, 138 (2013) 429.
22. J. Tian, Q. Liu, J. Shi, J. Hu, A. M. Asiri, X. Sun and Y. He, *Biosens. Bioelectron.*, 71 (2015) 1.
23. C. Gong, J. Chen, Y. Shen, Y. Song, Y. Song and L. Wang, *RSC Adv.*, 6 (2016) 79798.
24. E. Gkaniatsou, C. Sicard, R. Ricoux, J.-P. Mahy, N. Steunou and C. Serre, *Mater. Horiz.*, 4 (2017) 55.
25. Y. Song, D. Cho, S. Venkateswarlu and M. Yoon, *RSC Adv.*, 7 (2017) 10592.
26. J. Yang, H. Ye, Z. Zhang, F. Zhao and B. Zeng, *Sens. Actuators, B,* 242 (2017) 728.
27. Y. Chen and S. Ma, *Dalton Trans.*, 45 (2016) 9744.
28. D. Feng, T. F. Liu, J. Su, M. Bosch, Z. Wei, W. Wan, D. Yuan, Y. P. Chen, X. Wang, K. Wang, X. Lian, Z. Y. Gu, J. Park, X. Zou and H. C. Zhou, *Nat. Commun.*, 6 (2015) 5979.
29. J. Park, D. Feng and H. C. Zhou, *J. Am. Chem. Soc.*, 137 (2015) 11801.
30. J. Park, D. Feng and H. C. Zhou, *J. Am. Chem. Soc.*, 137 (2015) 1663.
31. E. C. Vermisoglou, T. Giannakopoulou, G. Romanos, N. Boukos, V. Psycharis, C. Lei, C. Lekakou, D. Petridis and C. Trapalis, *Appl. Surf. Sci.*, 392 (2017) 244.
32. Y. Li, L. Shi, G. Han, Y. Xiao and W. Zhou, *Sens. Actuators, B,* 238 (2017) 945.
33. S. Pakapongpan and R. P. Poo-arporn, *Mater. Sci. Eng. C*, (2017), doi: 10.1016/j.msec.
34. C. Liu, Q. Cai, B. Xu, W. Zhu, L. Zhang, J. Zhao and X. Chen, *Biosens. Bioelectron.*, 94 (2017) 200
35. S. Wu, F. Su, X. Dong, C. Ma, L. Pang, D. Peng, M. Wang, L. He and Z. Zhang, *Appl. Surf. Sci.*, 401 (2017) 262.

36. H. Liu, K. Guo, J. Lv, Y. Gao, C. Duan, L. Deng and Z. Zhu, *Sens. Actuators, B*, 238 (2017) 249.
37. J. G. Kleingardner, B. Kandemir and K. L. Bren, *J. Am. Chem. Soc.*, 136 (2014) 4.
38. B. Zhang, J. Zhou, S. Li, X. Zhang, D. Huang, Y. He, M. Wang, G. Yang and Y. Shen, *Talanta*, 131 (2015) 243.
39. B. Neumann, P. Kielb, L. Rustam, A. Fischer, I. M. Weidinger and U. Wollenberger, *ChemElectroChem*, (2017), doi: 10.1002/celc.201600776.
40. V. Lykourinou, Y. Chen, X. S. Wang, L. Meng, T. Hoang, L. J. Ming, R. L. Musselman and S. Ma, *J. Am. Chem. Soc.*, 133 (2011) 10382.
41. M. B. Majewski, A. J. Howarth, P. Li, M. R. Wasielewski, J. T. Hupp and O. K. Farha, *CrystEngComm*, (2017), doi: 10.1039/c7ce00022g.
42. T. Wang, J. Liu, J. Ren, J. Wang and E. Wang, *Talanta*, 143 (2015) 438.
43. S. Tian, Q. Zhou, Z. Gu, X. Gu, L. Zhao, Y. Li and J. Zheng, *Talanta*, 107 (2013) 324.
44. Y. Zhou, S. Liu, H. Jiang, H. Yang and H. Chen, *Electroanalysis*, 22 (2010) 1323.
45. J. Graca, R. Oliveira, M. Moraes and M. Ferreira, *Bioelectrochemistry*, 96 (2014) 37.
46. C. Gong, J. Chen, Y. Shen, Y. Song, Y. Song and L. Wang, *RSC Adv.*, 6 (2016) 79798.

© 2017 The Authors. Published by ESG (www.electrochemsci.org). This article is an open access article distributed under the terms and conditions of the Creative Commons Attribution license (http://creativecommons.org/licenses/by/4.0/).